Aerogel Electrocatalysts

DOI: 10.1002/anie.201108575

High-Performance Electrocatalysis on Palladium Aerogels**

*Wei Liu, Anne-Kristin Herrmann, Dorin Geiger, Lars Borchardt, Frank Simon, Stefan Kaskel, Nikolai Gaponik, and Alexander Eychmüller**

Novel self-assembled architectures are currently of great interest for nanochemistry and nanotechnology. Aerogels, a unique class of inorganic polymers with low densities, large open pores, and high inner surface areas, are well known for their superior physical and chemical properties, which are linked to their combination of specific properties of the nanomaterials magnified by self-assembly on the macroscale. Up to now, a wealth of research has been carried out on oxide-based aerogels, with the traditional silica, alumina, and titania aerogels amongst the most widely studied systems. These materials have found attractive applications, for example as thermal insulators and components of electrochemical devices.[1] A great deal of research has also been conducted on hybrid aerogels of metal nanoparticles (e.g. platinum) supported on aerogels (silica, titania, alumina, carbon, etc.), which combine both the catalytic properties of the metal nanoparticles and the highly porous structures of the aerogels.[2] Recently, the extension of sol–gel methods to the preparation of chalcogenide aerogels was realized.[3] Most recently, Leventis et al. has developed metal aerogels (including Fe, Co, Ni, Cu) by a carbothermal method.[4] Our group has developed nonsupported monometallic (Pt, Au, and Ag) and bimetallic (PtAg and AuAg) aerogels,[5] and composite aerogels of both semiconductor and metal nanoparticles have been successfully realized.[6] These aerogels formed from chalcogenide semiconductor or metal nanocrystals constitute an evolving class of materials with enormous potential on account of their optical and catalytic properties;[3–6] however, applications of these materials are still to be explored in width and depth.[3e] In addition, it is of great interest to develop new nanostructured metallic aerogels with high porosity, large surface area, and high activity by simple strategies. Previously, other important strategies have been developed to generate porous metal nanostructures, for example, by templating, dealloying, electrodepositing approaches;[7] recently, Krishna et al. have also reported a rapid synthesis of high-surface-area noble metal nanosponges by simply mixing the precursors and reducing agent.[8]

Cyclodextrins (CDs), a class of readily available, water-soluble, and nontoxic cyclic oligosaccharides with a hydrophobic inner cavity and a hydrophilic exterior, are of great importance in studies of host–guest interactions, molecular recognition, and drug delivery.[9] They have also drawn attention in the area of metal nanomaterials, mainly because they can enhance water-solubility properties and control particle size of nanoparticles. In contrast, not much attention has been paid to improving the catalytic activity of the metal nanoparticles by utilizing the host–guest interactions between cyclodextrin and the target molecules.[10]

Herein, we report a facile method to prepare nanostructured Pd aerogels modified by α-, β-, or γ-cyclodextrins (Pd_{CD}). When potassium tetrachloropalladate (K_2PdCl_4) was reduced with sodium borohydride ($NaBH_4$) in the presence of α-, β-, or γ-CD, the Pd_{CD} hydrogels formed spontaneously without additional treatment, and after subsequent drying with supercritical CO_2, Pd_{CD} aerogels were obtained. Using this simple approach, we produced Pd_{CD} aerogels with high porosities and large surface areas. The Pd_{CD} aerogels exhibit very high activities towards the electrooxidation of ethanol, with $Pd_{\alpha\text{-}CD}$ and $Pd_{\beta\text{-}CD}$ aerogels as the superior catalysts. Because of the simple and environmentally friendly preparation process together with the high catalytic activity, upscaling production of the Pd aerogels for commercial use is promising. The schematic illustration of the electrooxidation along with a picture of bits of $Pd_{\beta\text{-}CD}$ aerogel is shown in Scheme 1.

The evolving structures of the Pd_{CD} aerogels are highly porous and composed of interconnected networks of Pd nanowires. Figure 1 shows scanning electron microscopy (SEM) and transmission electron microscopy (TEM) images of the as-prepared $Pd_{\beta\text{-}CD}$ aerogel. The aerogel has a porous network structure composed of ultrathin primary nanowires with relatively uniform diameter of (3.6 ± 1) nm. These primary nanowires are fused and interconnected at various angles, while some are connected along the nanowire direction forming a branch-type structure. High-resolution transmission electron microscopy (HRTEM) images and the

[*] Dr. W. Liu, A.-K. Herrmann, Dr. N. Gaponik, Prof. A. Eychmüller
Physical Chemistry/Electrochemistry
Technical University of Dresden
Bergstrasse 66b, 01062 Dresden (Germany)
E-mail: alexander.eychmueller@chemie.tu-dresden.de
Homepage: http://www.chm.tu-dresden.de/pc2/eindex.shtml
Dr. D. Geiger
Triebenberg Laboratory for HRTEM and Electron Holography
Institute for Structure Physics, Technical University of Dresden
Zum Triebenberg 50, 01328 Dresden (Germany)
L. Borchardt, Prof. S. Kaskel
Inorganic Chemistry, Technical University of Dresden
Bergstrasse 66b, 01062 Dresden (Germany)
Dr. F. Simon
Physical Chemistry and Physics of Polymers
Leibniz Institute of Polymer Research Dresden
Hohe Strasse 6, 01069 Dresden (Germany)

[**] W.L. acknowledges support from the Alexander von Humboldt Foundation. This work was supported in part by DFG project EY16/10-2. We thank Ellen Kern for the SEM measurements and Stephen Hickey, Jan Poppe, Stefanie Tscharntke, Aliaksei Dubavik, Christoph Ziegler, Tobias Otto, Vladimir Lesnyak, and Thomas Hendel for their discussions and help.

Supporting information for this article is available on the WWW under http://dx.doi.org/10.1002/anie.201108575.

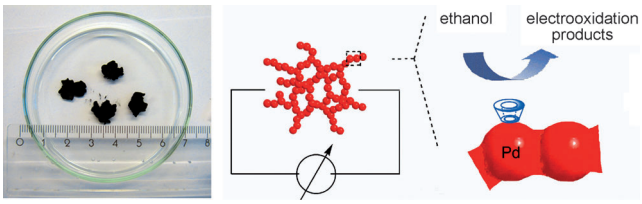

Scheme 1. Illustration of the electrocatalytic performance of the cyclodextrin-modified palladium aerogel in the oxidation of ethanol. The photograph shows bits of a $Pd_{\beta\text{-CD}}$ aerogel.

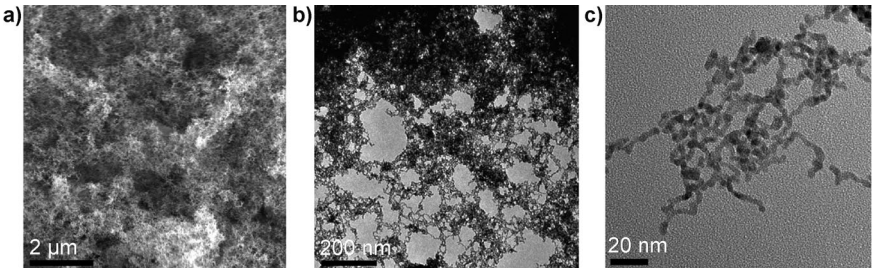

Figure 1. a) SEM image and b,c) TEM images of the $Pd_{\beta\text{-CD}}$ aerogel at different magnifications.

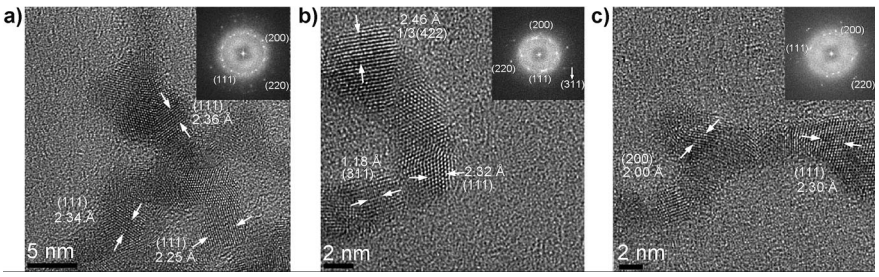

Figure 2. HRTEM images of the $Pd_{\beta\text{-CD}}$ aerogel: a) one cross-linked point, b) one curved turning part, and c) one nanowire with free branch ends of the $Pd_{\beta\text{-CD}}$ aerogel. The insets are their corresponding fast Fourier transformations (FFT).

corresponding fast Fourier transformations (FFTs) of some typical spots including one cross-linked point, one curved turning part, and a nanowire with free branch ends are shown in Figure 2. All the images show that the Pd nanowire networks are highly crystalline with a face-centered-cubic (fcc) polycrystalline structure. The crystalline domains containing lattice planes with interplanar distances of about 2.30 Å are assigned to the (111) plane of fcc metallic Pd, and are widely distributed at all locations. The kinetically forbidden 1/3(422) planes of fcc Pd with an interplanar spacing of 2.46 Å are also observed.[11] The fcc crystalline structure of the $Pd_{\beta\text{-CD}}$ aerogel is further confirmed by the X-ray powder diffraction pattern (Figure S1 in the Supporting Information). No signal from β-CD is detected, indicating the amorphous state of β-CD in the $Pd_{\beta\text{-CD}}$ aerogel.

$Pd_{\alpha\text{-CD}}$ and $Pd_{\gamma\text{-CD}}$ aerogels can be obtained by the same synthetic route. Their nanostructures are similar to that of the $Pd_{\beta\text{-CD}}$ aerogel (Figure S2). The average bulk density of the $Pd_{\beta\text{-CD}}$ aerogel is about 0.066 $g\,cm^{-3}$, which corresponds to approximately 1/182 of the bulk density of palladium.

The $Pd_{\beta\text{-CD}}$ aerogel was characterized by X-ray photoelectron spectroscopy, FTIR spectroscopy, energy-dispersive X-ray spectroscopy, and thermogravimetry analysis (Figure S3–S6). These analyses indicate that the $Pd_{\beta\text{-CD}}$ aerogel consists of two main components (about 56 wt% of Pd and about 44 wt% of β-CD), the Pd is mainly zero valent, and the porous Pd aerogel nanowire network surface is capped with β-CD molecules.

Information on the surface area and porosity properties of the $Pd_{\beta\text{-CD}}$ aerogel was obtained by analysis of its N_2 physisorption isotherm (Figure 3). The N_2 physisorption isotherm is essentially a combination of a type II and a type IV curve. The surface area determined by fitting the data to a Brunauer–Emmett–Teller (BET) isotherm is 92 $m^2 g^{-1}$ (molar surface area 16.64×10^3 $m^2 mol^{-1}$). Typical silica aerogels have a molar surface area of 30×10^3 $m^2 mol^{-1}$ and a maximum of roughly 10×10^4 $m^2 mol^{-1}$.[5] The surface area of the Pd aerogels greatly exceeds that of palladium nanowires synthesized in hexagonal mesophases[12] and that of interconnected hierarchical porous palladium nanostructures.[13]

The pore size distribution of the $Pd_{\beta\text{-CD}}$ aerogel was assessed using the quenched solid density functional theory (QSDFT) equilibrium model (N_2 on carbon) based on a slit-shaped pore geometry. The pore size distribution in Figure 3b shows the presence of a broad range of pores from micropores (< 2 nm) to mesopores (2–50 nm). Additionally, the absence of a plateau at high relative pressure P/P_0 in the

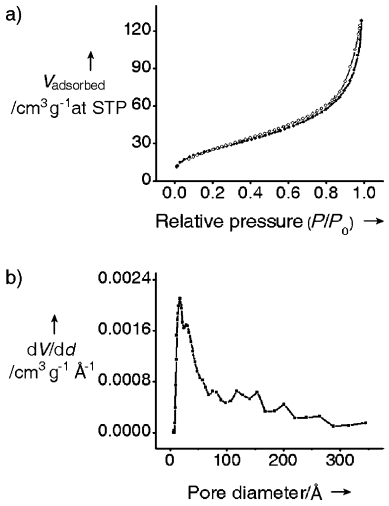

Figure 3. a) N_2 physisorption isotherm of the $Pd_{\beta\text{-CD}}$ aerogel; b) pore size distribution determined from the isotherm using the QSDFT equilibrium model (N_2 on carbon kernel) based on a slit-shaped pore geometry. The sample was degassed overnight at 323 K before testing.

adsorption isotherm implies the simultaneous presence of macropores (pore diameter > 50 nm).[3e,14] The presence of meso- and macropores in the aerogel is also evident in the above SEM and TEM images. The hierarchical porous structure of the Pd aerogel may enable faster diffusion of target molecules during catalysis. The existence of many micropores with the maximum at 1.8 nm may be a result of the high content of β-CD in the $Pd_{\beta\text{-CD}}$ aerogel.[15]

The cumulative pore volume for the $Pd_{\beta\text{-CD}}$ aerogel determined from the amount of adsorbed nitrogen at the relative pressure $P/P_0 = 0.985$ is 0.2 $cm^3 g^{-1}$. The micropore volume is determined to be 0.02 $cm^3 g^{-1}$ and the surface area for the micropores is 31 $m^2 g^{-1}$. The micropore volume is in agreement with the calculated value of 0.06 $cm^3 g^{-1}$ for an aerogel with 44 wt% of β-CD (cavity volume of β-CD 0.14 $cm^3 g^{-1}$),[16] considering that some β-CD cavities may not be accessible for the N_2 physisorption. The surface area of Pd would be 51.8 m^2 in 1 g of $Pd_{\beta\text{-CD}}$ aerogel, estimated by assuming a long network of Pd nanowires 3.6 nm in diameter and by using the Pd density of 12.023 g cm^{-3}. The coverage of this estimated Pd surface by one monolayer of β-CD (outer diameter of β-CD: 1.53 nm)[16] would need about 0.54 g of β-CD, more than the weight of about 0.44 g of β-CD in 1 g of $Pd_{\beta\text{-CD}}$ aerogel. These rough estimations may indicate that the surface of Pd is not fully covered by β-CD.

TEM and UV/Vis spectroscopy were conducted to monitor the formation process of the $Pd_{\beta\text{-CD}}$ hydrogel (Figures S7 and S8). The results show that the evolution of the $Pd_{\beta\text{-CD}}$ hydrogel involves four main stages, namely, the formation of Pd nanoparticles, short Pd nanowires, Pd nanowire networks and eventually the Pd hydrogel. These results are in good agreement with our observations during the synthesis (Figure S9). Control experiments, including reduction of K_2PdCl_4 directly by $NaBH_4$ without β-CD (Figure S10), indicate that the formation of the $Pd_{\beta\text{-CD}}$ hydrogel proceeds by a spontaneous assembly process. The in situ rapidly generated salts increase the ionic strength of the reaction solution and decrease the electrostatic repulsion between the primary Pd nanoparticles; they may also transform the isotropic electrostatic repulsions between the Pd nanoparticles into anisotropic forms, leading to the rapid anisotropic agglomeration of the colloidal Pd nanoparticles. When β-CD molecules are present during the synthesis, they cap the surface of the Pd nanoparticles and provide repulsive steric interactions, which reduce the size distribution and slow down the assembly of the Pd nanoparticles. The presence of a large amount of β-CD molecules may also lower the dielectric constant of the reaction solution ($\varepsilon_{H_2O} = 80.1$, $\varepsilon_{\beta\text{-CD}} = 52.0$) and decrease the surface charge of the Pd particles ($\xi_{no\,\beta\text{-CD}} = -26.4$ mV, $\xi_{with\,\beta\text{-CD}} = -21.4$ mV, measured at 2 h reaction time), resulting in the formation of a large amount of long fused Pd nanowires.[17] We are still studying the formation mechanism of the Pd_{CD} hydrogels.

Pd is widely known for its remarkably high activity towards ethanol electrooxidation in alkaline solution.[18] The electrocatalytic performances of the nanoporous Pd_{CD} aerogels toward ethanol oxidation were evaluated by cyclic voltammetry (CV) and chronoamperometry in a 1 M KOH aqueous solution containing 1 M C_2H_5OH (Figure 4). Commercial palladium supported on carbon (Pd/C, 10 wt%) was also tested for comparison. The electrochemically active surface area (ECSA) of the Pd_{CD} aerogels and the Pd/C electrodes were estimated using the reduction charge of $Pd(OH)_2$ obtained from the CVs of the electrodes in 0.5 M H_2SO_4 in the range of −0.4 V–1.04 V (vs Ag/AgCl) (Figure S11).[19] The potential limit at 1.04 V was chosen according to the Pourbaix pH–potential diagram for the upper limit of the formation of $Pd(OH)_2$ in a solution of pH 0.[19] The reported minimum charge density value of 430 μC cm^{-2} for the formation of a fully covered $Pd(OH)_2$ layer on typical single-crystal Pd surfaces was used for the ECSA calculation.[19] The possible deviation of this charge-to-surface-area conversion might lead to an overestimate of the ECSA.[19] The evaluated ECSA values for the $Pd_{\alpha\text{-CD}}$, $Pd_{\beta\text{-CD}}$, $Pd_{\gamma\text{-CD}}$ aerogels and Pd/C are 98, 69, 51, 57 $m^2 g^{-1}$, respectively. The electrocatalytic activities of the Pd_{CD} aerogels and the Pd/C catalysts toward ethanol oxidation obtained from Figure 4, top, and some Pd nanomaterials reported in literatures are summar-

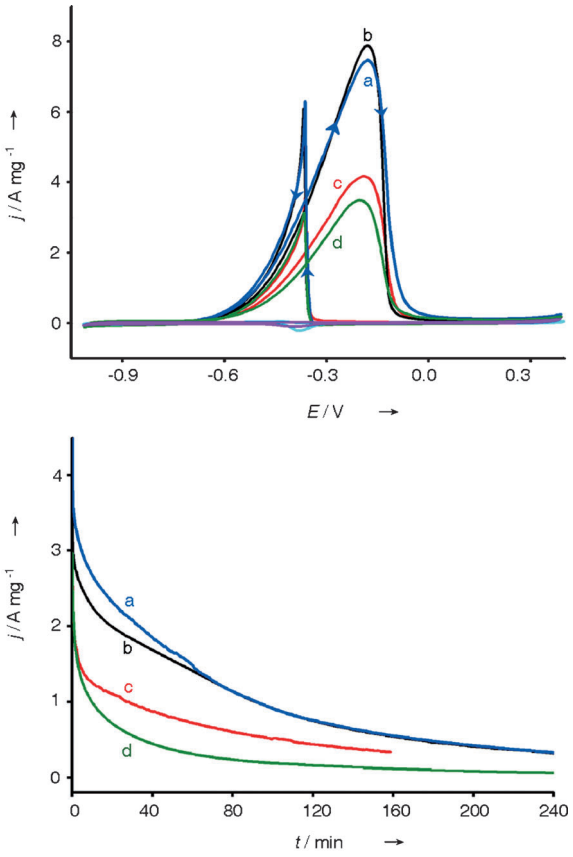

Figure 4. Top: Cyclic voltammograms (CV) of electrodes modified with a) $Pd_{\alpha\text{-CD}}$, b) $Pd_{\beta\text{-CD}}$, and c) $Pd_{\gamma\text{-CD}}$ aerogels, and modified with d) Pd/C in 1.0 M KOH + 1.0 M C_2H_5OH aqueous solution in the potential range of −1.0 V–0.4 V versus Ag/AgCl (3 M NaCl). Scan rate: 50 $mV s^{-1}$. CV of electrodes modified with $Pd_{\beta\text{-CD}}$ (light blue) and Pd/C (magenta) in 1.0 M KOH aqueous solution. Bottom: Chronoamperometric curves for ethanol electrooxidation at −0.3 V on the a) $Pd_{\alpha\text{-CD}}$, b) $Pd_{\beta\text{-CD}}$, and c) $Pd_{\gamma\text{-CD}}$ aerogels, and the d) Pd/C-modified electrodes in 1.0 M KOH + 1.0 M C_2H_5OH aqueous solution. Loading amount of Pd: 20 μg cm^{-2}.

ized in Table S1 for comparison. Figure 4, top, is enlarged and shown in Figure S12 for better resolution.

All the cyclic voltammograms of the Pd_{CD} aerogels and the Pd/C electrodes show two well-defined current peaks characteristic of the electrooxidation of alcohol. In contrast, only very weak responses corresponding to the Pd oxidation/reduction and H evolution can be seen in 1M KOH aqueous solution without ethanol (Figure 4, top, and Figure S13). The generally accepted mechanism for ethanol electrooxidation in alkaline media is shown in Equations S(1)–S(4).[12,18c] The peak current of the forward scan is related to the oxidation of freshly chemisorbed species from the ethanol adsorption. The sharp anodic oxidation current in the reverse scan represents the removal of carbonaceous intermediate species not completely oxidized in the forward scan. A high I_f/I_b ratio indicates the efficient oxidation of alcohol during the forward anodic scan with little accumulation of carbonaceous residues. The values of the I_f/I_b ratio for the $Pd_{\alpha\text{-}CD}$, $Pd_{\beta\text{-}CD}$, $Pd_{\gamma\text{-}CD}$ aerogels and the Pd/C electrodes are 1.16, 1.28, 1.17, and 1.09, respectively, indicating more efficient ethanol electrooxidation and a lower chance of poisoning for the Pd_{CD} aerogels.

The onset potentials on the $Pd_{\alpha\text{-}CD}$, $Pd_{\beta\text{-}CD}$, and $Pd_{\gamma\text{-}CD}$ aerogels and the Pd/C electrodes are at −0.802 V, −0.816 V, −0.794 V, and −0.746 V, respectively. The 47–69 mV negative shift of the onset potentials of the $Pd_{\alpha\text{-}CD}$, $Pd_{\beta\text{-}CD}$, and $Pd_{\gamma\text{-}CD}$ aerogels relative to that of the Pd/C electrode indicates an enhancement in the kinetics of the ethanol electrooxidation for the Pd_{CD} aerogel. Notably, the current densities of the forward oxidation of ethanol on the Pd_{CD} aerogels, especially the $Pd_{\alpha\text{-}CD}$ and $Pd_{\beta\text{-}CD}$ aerogels, are amazingly high: 7.388 A mg^{-1} Pd, 7.830 A mg^{-1} Pd, and 4.119 A mg^{-1} Pd for the $Pd_{\alpha\text{-}CD}$, $Pd_{\beta\text{-}CD}$, and $Pd_{\gamma\text{-}CD}$ aerogels, respectively. The current densities of electrodes modified with $Pd_{\alpha\text{-}CD}$, $Pd_{\beta\text{-}CD}$, and $Pd_{\gamma\text{-}CD}$ aerogels are superior to those listed in Table S1 for nonsupported Pd nanomaterials and the various Pd/C materials. The current densities for the $Pd_{\alpha\text{-}CD}$, $Pd_{\beta\text{-}CD}$, and $Pd_{\gamma\text{-}CD}$ aerogels are 2.2, 2.3, and 1.2 times that of Pd/C in our test. The relationship between the anodic current density and the square root of the scan rate of the $Pd_{\beta\text{-}CD}$ aerogel and the Pd/C electrodes were investigated (Figure S14). The Pd/C electrode shows a linearship starting from 5 mV s^{-1}, while for the $Pd_{\beta\text{-}CD}$ aerogel the linearity starts at 20 mV s^{-1}. The results indicate that the electrooxidation of ethanol on Pd/C is controlled by mass transport through all the scan rates, while the $Pd_{\beta\text{-}CD}$ aerogel electrode is not controlled by mass transport until the scan rate is higher than 20 mV s^{-1}.[20]

The long-term stabilities of the nanoporous Pd_{CD} aerogels and the Pd/C electrodes were characterized by chronoamperometry in 1M KOH + 1M C_2H_5OH solution with a bias at −0.3 V (Figure 4, bottom). Initial rapid decay in current density was observed for all the electrodes, which may be due to the accumulation of strongly adsorbed poisoning intermediate species on the active sites. Subsequently, the current decreased slowly and reached a pseudo-steady state. The Pd_{CD} aerogels, especially the $Pd_{\alpha\text{-}CD}$ and $Pd_{\beta\text{-}CD}$ aerogels, exhibit much higher initial polarization current densities and slower current decays for the ethanol electrooxidation than the Pd/C electrode does. Among the Pd_{CD} aerogels, $Pd_{\alpha\text{-}CD}$ and $Pd_{\beta\text{-}CD}$ aerogels show similar performance with their current densities higher than that for the $Pd_{\gamma\text{-}CD}$ aerogel, which is in agreement with the CV results. The steady-state current densities of the $Pd_{\alpha\text{-}CD}$ and $Pd_{\beta\text{-}CD}$ aerogel electrodes at 30 min, 2 h, and 4 h test are about 3.6, 4.7, and 5.5 times that of the Pd/C electrode, respectively. These results further confirm the higher catalytic activity and better tolerance to the intermediate species of the Pd_{CD} aerogels toward ethanol electrooxidation.[20,21]

The very high electrocatalytic activity of the Pd_{CD} aerogels may be ascribed to the highly porous nonsupported ultrafine nanoassembly network structure of the aerogel. In contrast to Pd/C, the formation of irregular aggregates or agglomerations is largely avoided in the aerogel (Figure S15), which may favor the exposure of catalytic active sites and a good reactant flux resulting from the existence of many mesopores and micropores. In addition, the cyclodextrins may serve as an ethanol reservoir and enhance the electrocatalytic activity as a resulf of the host–guest interaction between the cyclodextrins and ethanol.[10,22] α-CD and β-CD are known to form inclusion complexes with alcohols, including ethanol, whereas in the case of γ-CD, only propanol has been found to form an inclusion complex.[23] Therefore, we suppose that the higher complexation ability of α-CD and β-CD to ethanol may be one reason for the superior performances of $Pd_{\alpha\text{-}CD}$ and $Pd_{\beta\text{-}CD}$ aerogels toward the oxidation of ethanol.

In summary, novel Pd aerogels modified with α, β, and γ-CD have been prepared by a facile method. By reducing K_2PdCl_4 with $NaBH_4$ in the presence of α-, β-, or γ-CD, the Pd hydrogels formed spontaneously without additional treatments, and after subsequent drying with supercritical CO_2 freestanding Pd aerogels were obtained. The Pd aerogels show strikingly high electrocatalytic activities toward the oxidation of ethanol in alkaline solution. This work sheds bright light on potential applications of metallic aerogel-based catalysts for example in lightweight high-performance fuel cells.

Received: December 5, 2011
Revised: January 30, 2012
Published online: April 24, 2012

Keywords: aerogels · cyclodextrins · electrocatalysis · ethanol · palladium

[1] a) S. S. Kistler, *Nature* **1931**, *127*, 741 – 741; b) H. D. Gesser, P. C. Goswami, *Chem. Rev.* **1989**, *89*, 765 – 788; c) N. Hüsing, U. Schubert, *Angew. Chem.* **1998**, *110*, 22 – 47; *Angew. Chem. Int. Ed.* **1998**, *37*, 22 – 45; d) D. R. Rolison, B. Dunn, *J. Mater. Chem.* **2001**, *11*, 963 – 980.

[2] a) G. M. Pajonk, *Catal. Today* **1997**, *35*, 319 – 337; b) S. Wei, D. Wu, X. Shang, R. Fu, *Energy Fuels* **2009**, *23*, 908 – 911; c) C. Sotiriou-Leventis, X. Wang, S. Mulik, A. Thangavel, N. Leventis, *Synth. Commun.* **2008**, *38*, 2285 – 2298.

[3] a) J. L. Mohanan, I. U. Arachchige, S. L. Brock, *Science* **2005**, *307*, 397 – 400; b) A. Eychmüller, *Angew. Chem. Int. Ed.* **2005**, *44*, 4839 – 4841; c) I. U. Arachchige, S. L. Brock, K. K. Kalebaila, *Comments Inorg. Chem.* **2006**, *27*, 103 – 126; d) I. U. Arachchige, S. L. Brock, *J. Am. Chem. Soc.* **2006**, *128*, 7964 – 7971; e) S. Bag, P. N. Trikalitis, P. J. Chupas, G. S. Armatas, M. G. Kanatzidis,

Science **2007**, *317*, 490 – 493; f) S. Bag, M. G. Kanatzidis, *J. Am. Chem. Soc.* **2008**, *130*, 8366 – 8376; g) I. U. Arachchige, S. L. Brock, *Acc. Chem. Res.* **2007**, *40*, 801 – 809; h) N. Gaponik, A. Wolf, R. Marx, V. Lesnyak, K. Schilling, A. Eychmüller, *Adv. Mater.* **2008**, *20*, 4257 – 4262.

[4] a) N. Leventis, N. Chandrasekaran, C. Sotiriou-Leventis, A. Mumtaz, *J. Mater. Chem.* **2009**, *19*, 63 – 65; b) N. Leventis, N. Chandrasekaran, A. G. Sadekar, C. Sotiriou-Leventis, H. Lu, *J. Am. Chem. Soc.* **2009**, *131*, 4576 – 4577; c) N. Leventis, N. Chandrasekaran, A. G. Sadekar, S. Mulik, C. Sotiriou-Leventis, *J. Mater. Chem.* **2010**, *20*, 7456 – 7471.

[5] N. C. Bigall, A.-K. Herrmann, M. Vogel, M. Rose, P. Simon, W. Carrillo-Cabrera, D. Dorfs, S. Kaskel, N. Gaponik, A. Eychmüller, *Angew. Chem.* **2009**, *121*, 9911 – 9915; *Angew. Chem. Int. Ed.* **2009**, *48*, 9731 – 9734.

[6] V. Lesnyak, A. Wolf, A. Dubavik, L. Borchardt, S. V. Voitekhovich, N. Gaponik, S. Kaskel, A. Eychmuller, *J. Am. Chem. Soc.* **2011**, *133*, 13413 – 13420.

[7] a) B. C. Tappan, S. A. Steiner III, E. P. Luther, *Angew. Chem.* **2010**, *122*, 4648 – 4669; *Angew. Chem. Int. Ed.* **2010**, *49*, 4544 – 4565; b) S. Cherevko, N. Kulyk, C.-H. Chung, *Nanoscale* **2012**, *4*, 103 – 105.

[8] K. S. Krishna, C. S. S. Sandeep, R. Philip, M. Eswaramoorthy, *ACS Nano* **2010**, *4*, 2681 – 2688.

[9] a) G. Wenz, B.-H. Han, A. Müller, *Chem. Rev.* **2006**, *106*, 782 – 817; b) K. Uekama, F. Hirayama, T. Irie, *Chem. Rev.* **1998**, *98*, 2045 – 2076; c) W. Liu, Y. Zhang, X. Gao, *J. Am. Chem. Soc.* **2007**, *129*, 4973 – 4980.

[10] K. Mori, N. Yoshioka, Y. Kondo, T. Takeuchi, H. Yamashita, *Green Chem.* **2009**, *11*, 1337 – 1342.

[11] X. Huang, S. Tang, X. Mu, Y. Dai, G. Chen, Z. Zhou, F. Ruan, Z. Yang, N. Zheng, *Nat. Nanotechnol.* **2011**, *6*, 28 – 32.

[12] F. Ksar, G. Surendran, L. Ramos, B. Keita, L. Nadjo, E. Prouzet, P. Beaunier, A. Hagege, F. Audonnet, H. Remita, *Chem. Mater.* **2009**, *21*, 1612 – 1617.

[13] A. Halder, S. Patra, B. Viswanath, N. Munichandraiah, N. Ravishankar, *Nanoscale* **2011**, *3*, 725 – 730.

[14] K. S. W. Sing, D. H. Everett, R. A. W. Haul, L. Moscou, R. A. Pierotti, J. Rouquerol, T. Siemieniewska, *Pure Appl. Chem.* **1985**, *57*, 603 – 619.

[15] S. Polarz, B. Smarsly, L. Bronstein, M. Antonietti, *Angew. Chem.* **2001**, *113*, 4549 – 4553; *Angew. Chem. Int. Ed.* **2001**, *40*, 4417 – 4421.

[16] J. Szejtli, *Chem. Rev.* **1998**, *98*, 1743 – 1753.

[17] a) H. Zhang, D. Wang, *Angew. Chem.* **2008**, *120*, 4048 – 4051; *Angew. Chem. Int. Ed.* **2008**, *47*, 3984 – 3987; b) J. Xie, Q. Zhang, J. Y. Lee, D. I. C. Wang, *J. Phys. Chem. C* **2007**, *111*, 17158 – 17162.

[18] a) E. Antolini, *Energy Environ. Sci.* **2009**, *2*, 915 – 931; b) E. Antolini, E. R. Gonzalez, *J. Power Sources* **2010**, *195*, 3431 – 3450; c) C. Bianchini, P. K. Shen, *Chem. Rev.* **2009**, *109*, 4183 – 4206.

[19] a) M. J. N. Pourbaix, J. Van Muylder, N. de Zoubov, *Platinum Met. Rev.* **1959**, *3*, 100 – 106; b) L. Xiao, L. Zhuang, Y. Liu, J. Lu, H. D. Abruña, *J. Am. Chem. Soc.* **2009**, *131*, 602 – 608.

[20] F. Hu, X. Cui, W. Chen, *J. Phys. Chem. C* **2010**, *114*, 20284 – 20289.

[21] a) C. Xu, L. Cheng, P. Shen, Y. Liu, *Electrochem. Commun.* **2007**, *9*, 997 – 1001; b) F. Ksar, L. Ramos, B. Keita, L. Nadjo, P. Beaunier, H. Remita, *Chem. Mater.* **2009**, *21*, 3677 – 3683.

[22] a) T. Aree, N. Chaichit, *Carbohydr. Res.* **2003**, *338*, 1581 – 1589; b) J. N. Spencer, J. DeGarmo, I. M. Paul, Q. He, X. Ke, Z. Wu, C. H. Yoder, S. Chen, J. E. Mihalick, *J. Solution Chem.* **1995**, *24*, 601 – 609; c) T. Aree, N. Chaichit, *Carbohydr. Res.* **2008**, *343*, 2285 – 2291; d) J. Pitha, T. Hoshino, *Int. J. Pharm.* **1992**, *80*, 243 – 251; e) Y. Matsui, K. Mochida, *Bull. Chem. Soc. Jpn.* **1979**, *52*, 2808 – 2814.

[23] a) J. Ding, T. Steiner, W. Saenger, *Acta Crystallogr. Sect. B* **1991**, *47*, 731 – 738; b) K. Lindner, W. Saenger, *Biochem. Biophys. Res. Commun.* **1980**, *92*, 933 – 938.

